PHILOSOPHICAL TRANSACTIONS OF THE ROYAL SOCIETY A MATHEMATICAL, PHYSICAL & ENGINEERING SCIENCES

The dynamics of extensional sedimentary basins: constraints from subsidence inversion

Robert Newman and Nicky White

Phil. Trans. R. Soc. Lond. A 1999 **357**, 805-834
doi: 10.1098/rsta.1999.0353

THE ROYAL SOCIETY

The dynamics of extensional sedimentary basins: constraints from subsidence inversion

By Robert Newman and Nicky White

Bullard Laboratories, Madingley Rise, Madingley Road, Cambridge CB3 0EZ, UK

On the continents, sedimentary basins are generally formed by small amounts of lithospheric extension. Extension might cease because the lithospheric mantle has cooled and strengthened, or because the driving force is removed. In the former case, a relationship should exist between the maximum strain rate during extension and the final stretching factor attained. We explore how this relationship depends on the rheology of the lithospheric mantle and of the crust, as well as on sedimentation and prior rifting events. We also present strain rate information obtained by inverting subsidence data from a variety of sedimentary basins. There is evidence of a systematic relationship between strain rate and stretching factor in each basin, implying that lithospheric rheology is consistent with the rheology of olivine measured in laboratory experiments. Our data are difficult to explain if removal of the driving force governs the magnitude of stretching factors.

Keywords: lithosphere; geometrical inversion; strain rate; rheology; rifting; subsidence

1. Introduction

Extension of the continental lithosphere is widespread, but the dynamics of this process are still not well understood. Several models have been developed which make assumptions about the forces driving extension and about the rheology of the lithosphere, which together determine the spatial and temporal distribution of strain. The usefulness of these dynamical models has been limited by uncertainties in extrapolating laboratory-derived rheologies to geological strain rates. Furthermore, little attempt has been made to constrain the models by independent kinematic observations.

A particularly important question is what determines the final stretching factor. The effective viscosity of rocks is strongly dependent on temperature and this dependence led England (1983) to propose that cooling of the lithospheric mantle and a corresponding increase in its viscosity cause extension to stop. Since temperature changes depend upon strain rate, there is a characteristic relationship between initial strain rate and final stretching factor. Sonder & England (1989) showed that there is evidence of this mechanism operating in the Aegean, where areas with high stretching factors currently have relatively low present-day strain rates.

The approach used by England (1983, 1986), Houseman & England (1986) and Kusznir & Park (1987) was one-dimensional, but the effect of temperature changes on viscosity has also been included in two-dimensional models (e.g. Keen 1985; Braun & Beaumont 1987; Dunbar & Sawyer 1989; Bassi 1991, 1995; Christensen 1992; Bassi

et al. 1993; Ruppel, 1995). Most of these two-dimensional models focus attention on the spatial distribution of strain rather than on variation of strain rate with time. Results depend on the exact details of each model and it is not always clear which parameters are most significant. Buck (1991) differentiates between a 'wide rift mode' of extension, where cooling and strengthening of the lithosphere is important, and a 'narrow rift mode', where it is not. He also defines a 'core complex mode', where lower crustal flow is important. He finds that the wide rift mode is favoured by high Moho temperatures (greater than 800 °C), but he imposes strain rates rather than calculating them.

One way of testing different models is to compare their predictions with the observed temporal variation of strain rates in extensional sedimentary basins. To achieve this end, we exploit the fact that subsidence data from the basins should indirectly record strain rate history. When modelling subsidence, extension is usually assumed to be instantaneous (McKenzie 1978) or to occur at a constant rate for a specific period of time (Jarvis & McKenzie 1980). Recently, White (1993, 1994) has developed a method for inverting subsidence curves, which has now been applied to many different basins. In Newman & White (1997), we suggested that the relationship between peak strain rate and total stretching factor in these basins is indeed compatible with viscosity-controlled extension and that the pattern of results is more difficult to explain by force-controlled extension. We estimated that the rheology of lithospheric mantle is similar to that obtained by laboratory experiments on dry olivine, and proposed that some of the scatter in our strain rate data may be caused by the thermal effects of sedimentation and by prior stretching episodes.

In this paper, we analyse the dynamics of viscosity-controlled extension in more detail. First, we review the dynamical problem and use a simple two-dimensional model to justify a one-dimensional approach. Important complications such as sedimentation, crustal strength, brittle deformation, and variations in driving forces are discussed. Simple analytical approximations are given in support of our numerical results. We then show inverted strain rate data for several regions, and, finally, we discuss what the data reveal about the mechanics of extension and the rheology of the lithosphere.

2. The dynamical problem

(*a*) *Driving forces*

If an extensional force is applied to one side of a continental region, and the opposite side is fixed, extensional deviatoric stresses arise throughout the region. We refer to such forces as distant driving forces (Braun & Beaumont 1987); their exact origin is not important for understanding the deformation of the region, only their magnitude, direction, and the way in which they vary with time.

It is possible that variations in strain rate during extension are almost entirely caused by changes in the driving force and that extension stops when the driving force is removed. We refer to this behaviour as force-controlled extension. Since any variation in the force affects stresses throughout the whole region, one would expect to see increases and decreases in strain rate occurring at the same time, regardless of location. A similar situation arises if one boundary is constrained to move at a certain velocity in order to fit in with surrounding plate motions. In such a case,

time-dependent deviatoric stresses are still experienced across the region, the only difference being that the stress varies with time to produce the correct boundary velocity.

Buoyancy forces are generated when there are lateral density variations in the lithosphere such as crustal thickness variations (e.g. Artyushkov 1973). They assist extension where the crust is thick (or where the lithospheric mantle is thin) and oppose extension where the crust is thin. Buoyancy forces may therefore moderate the effects of a distant force. Extensional stress is reduced where the crust is thinned and, if buoyancy forces are sufficiently large, extension should stop completely once a certain crustal thickness is reached. If the lower crust is relatively weak, buoyancy forces can also result in lower crustal flow, which tends to reduce variations in crustal thickness (Buck 1991). It is also possible that buoyancy forces are the primary driving force for extension. For example, the crust may be relatively thick (Sonder *et al.* 1987), or the lithosphere may be elevated above hot mantle (Bott & Kusznir 1979), including mantle plumes (Houseman & England 1986). Jones *et al.* (1996) found that, in the western United States, areas of present-day extension do indeed have extensional buoyancy forces.

It is important to consider whether buoyancy forces can produce a correlation between strain rate and stretching factor without any significant changes in viscosity. The magnitude of buoyancy forces is approximately proportional to the square of the crustal thickness, so the strain rate in a situation where buoyancy forces stop extension can be estimated by

$$\dot{\epsilon}_{xx} = \frac{1}{8\mu L}\{2\tau_{\mathrm{o}} L_{\mathrm{o}} - \rho^* g(c_{\mathrm{o}}^2 - c^2)\}, \tag{2.1}$$

where τ_{o} is the deviatoric stress produced by the distant driving force, c_{o} and c are the original and current crustal thicknesses, L_{o} and L are the original and current lithospheric thicknesses, μ is a mean viscosity of the lithosphere (assumed to be independent of time here), and ρ^* is a density-related expression combining the effects of crustal thinning with those of thinning the lithospheric mantle (Newman 1992). In equation (2.1), the strain rate depends on the viscosity. The final stretching factor is reached when the term in braces is zero and does not depend on the viscosity. Thus there would be no correlation between the initial strain rate and the final stretching factor unless the viscosity was the same throughout the basin. For the same correlation to be observed in all sedimentary basins, the buoyancy forces as well as the viscosity would have to be the same in each basin, which is very unlikely to be the case. Jones *et al.* (1996), for example, conclude that there are considerable viscosity differences within the western United States.

A further means of generating extensional stresses is to apply shear stresses to the base of the lithosphere. These might represent the effect of convectional motion in the mantle, with extension occurring above diverging convective flow. The magnitude of such stresses is probably small because the combination of pressure and temperature in the asthenosphere gives it a very low viscosity. This low viscosity is predicated upon the continental lithosphere having a similar thermal structure as mature oceanic lithosphere. Our subsidence data are consistent with a 120 km thick plate, which has a basal temperature of 1330 °C (see figure 6), and so this thermal structure is probably appropriate.

(b) Lithospheric rheology

Information about rock rheology comes from laboratory experiments where rocks are deformed at high temperatures and pressures. Constitutive relationships are derived that express strain rate as a function of temperature, pressure, and deviatoric stress (Kirby & Kronenburg 1987). Application of laboratory results to the continental lithosphere depends on a range of important assumptions. Experimental strain rates are much faster than geological ones (less than $10^{-14}\ \mathrm{s}^{-1}$), samples are usually monomineralic rather than polyphase aggregates, and the effects of melt, hydrous phases and grain size are uncertain (Paterson 1987).

Nonetheless, laboratory results suggest that while the details of rheology are complicated, rocks under lithospheric conditions are most likely to obey a power law creep relationship unless they behave in a brittle manner (Brace & Kohlstedt 1980; Kohlstedt *et al*. 1995). For power-law creep,

$$\dot{\epsilon} = A\tau^n \exp(-Q/RT), \tag{2.2}$$

where $\dot{\epsilon}$ is the strain rate, τ is the deviatoric stress, T is the absolute temperature, R is the universal gas constant, and A, Q and n are material-dependent constants. The activation energy, Q, ranges from *ca.* 500 kJ mol^{-1} for dry olivine to *ca.* 160 kJ mol^{-1} for quartz and the power-law exponent, n, is in the range 3–5 (Kirby & Kronenburg 1987). This temperature dependence is the basis of viscosity-controlled extension. If extension takes more than 5 Ma, temperature changes of tens of degrees occur in the uppermost lithospheric mantle, changing the effective viscosity by at least an order of magnitude.

The viscosity of crustal material also increases as it cools, but because the crust is thinned its depth-integrated viscosity decreases. It is therefore unlikely that crustal strengthening can stop extension. When the geothermal gradient is restored to its stable condition, the temperature at a given depth might be slightly lower than it was before extension because of the redistribution of heat-producing elements, but thinning and hence weakening of the crust is more important during extension.

Brittle deformation is often assumed to obey Byerlee's law in which the stress required for brittle deformation increases linearly with depth (Byerlee 1968; Brace & Kohlstedt 1980). This law can be thought of as representing the stress required to overcome the frictional resistance to sliding on faults of all orientations. Most continental earthquakes occur in the upper 15 km of the crust (Meissner & Strehlau 1982; Chen & Molnar 1983), and so the mid-crustal level is regarded as the depth at which the brittle–plastic transition occurs. Earthquake stress drops, however, are not consistent with Byerlee's law (Frohlich 1989) and there is evidence from laboratory experiments of a zone of semibrittle deformation (Scholz 1990; Hirth & Tullis 1994; Kohlstedt *et al*. 1995), so the precise relationship between deviatoric stress and depth must be treated with caution.

(c) Strain distribution

It is now possible to measure directly velocities of the Earth's surface using methods such as Global Positioning System satellites (Billiris *et al*. 1991; Bennett *et al*. 1996) and satellite laser ranging (Smith *et al*. 1994). Seismic moment tensors of large earthquakes can also be used to estimate strain rates and are consistent with the direction but not always the magnitude of surface velocities (Jackson *et al*. 1992,

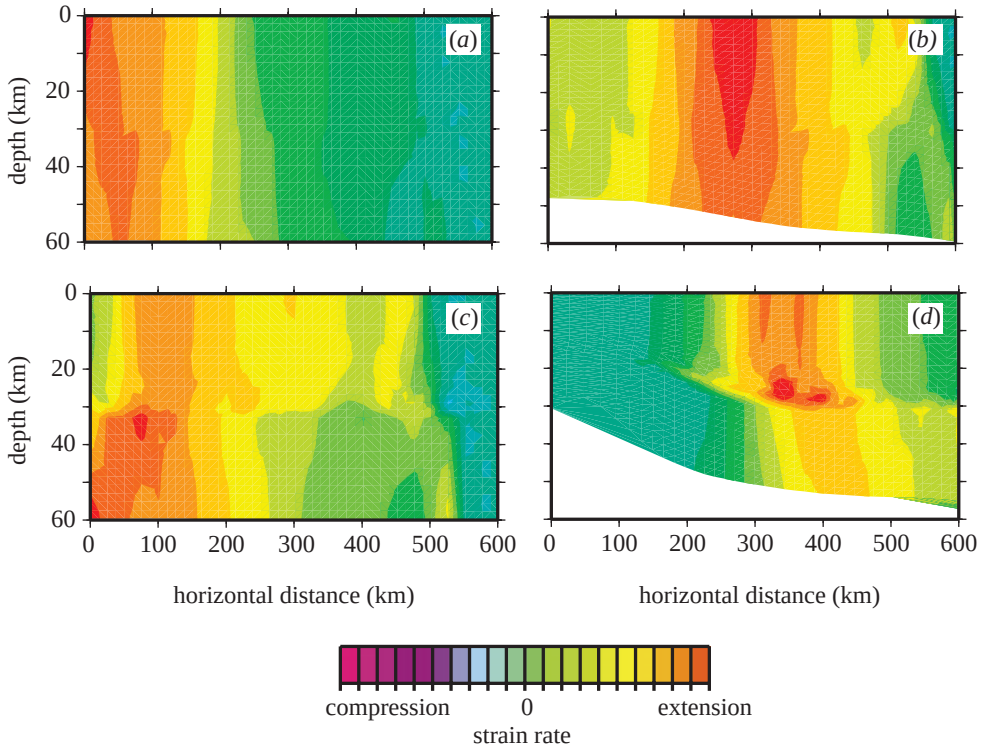

Figure 1. Contours of extensional strain rate, $\dot{\epsilon}_{xx}$, for two-dimensional experiments. Red represents the highest strain rates in each diagram and green represents zero strain rate. A constant driving force is applied at the right-hand boundary and the left-hand boundary is an axis of symmetry. Only the top half of the lithosphere is shown. Principal parameters for the experiments are given in table 1. Except for (*d*), the crust is initially 2 km thicker and the Moho 40 °C hotter near the left-hand boundary. (*a*) Crustal rheology has $Q_c = 300$ kJ mol^{-1}, $A_c = 10^{-19}$ Pa^{-3} s^{-1}, and $B = 0.25$; extension is just beginning. (*b*) Same experiment as (*a*) but 40 Ma after start of extension. (*c*) Rheology as in (*a*) except that $A_c = 10^{-15}$ Pa^{-3} s^{-1}; extension is just beginning. (*d*) Same rheology as (*c*) but the crustal heat production is higher rather than the crust being thicker near the left-hand boundary; 30 Ma after start of extension.

1994). It is much harder to obtain estimates of how strain rates vary over geological time-scales and the subsidence inversion discussed below is the best available method.

Two important questions about the distribution of strain must first be answered and present-day deformation helps with one of them: can the lithosphere be treated as a continuum (Thatcher 1995)? Upper crustal deformation is obviously discontinuous with many active faults of different orientations. It is possible that the brittle upper crust passively follows a strain rate distribution established within the plastic lower crust and lithospheric mantle. This view is supported by the diffuse nature of continental deformation: extension occurs on many faults over a broad area. For our purposes, viscosity-controlled extension implies that the plastic layers regulate strain rate so if the continuum approximation was invalid, we would not obtain a characteristic correlation between strain rate and stretching factor.

The second question is whether strain varies with depth. Subsidence in many basins can be modelled assuming pure shear extension (e.g. Barton & Wood 1984), but there are also basins where depth-dependent strain has been proposed (Royden & Keen 1980; Hellinger & Sclater 1983; White & McKenzie 1988). There is a considerable variation of viscosity with temperature and hence with depth, so some degree of depth-dependent strain is plausible. To address this issue, we will first examine deformation in a vertical plane.

3. A dynamical model

(a) *Numerical method*

Assuming that the continuum approximation is valid, we can solve the equation of motion,

$$\frac{\partial \sigma_{ij}}{\partial x_j} = -\rho g_i, \tag{3.1}$$

subject to the incompressibility condition, $\nabla \cdot v = 0$, for a suitably chosen rheology. We also need to solve the equation of thermal diffusion,

$$\rho c_p \frac{\partial T}{\partial t} = k\nabla^2 T + H, \tag{3.2}$$

where c_p is the specific heat capacity, k is the thermal conductivity and H is the rate of radioactive heat production. Since equations (3.1) and (3.2) are coupled and since the rheology can be complex, we use a finite-element method to solve for velocity and temperature at each point (Newman 1992). The lithosphere is represented by a grid of about 1000 triangular elements, each of which has six nodes. Continuous deformation is approximated by solving the equations as a series of boundary value problems representing the situation at intervals of *ca.* 0.5 Ma. Nodes are taken to be material points and are moved between time-steps according to their calculated velocities. Density and viscosity are adjusted according to the temperature; discontinuities in density and viscosity (e.g. at the Moho) remain sharply defined throughout the deformation.

Any rheology can be chosen for the lithosphere as long as an effective viscosity can be calculated to apply at each node. When more than one rheology is included, the operative rheology is taken to be the one that gives the lowest effective viscosity. As viscosity depends upon strain rate, the equation of motion is solved iteratively until strain rates converge to a solution satisfying the chosen rheology. If required, Byerlee's law is approximated by setting the viscosity to be

$$\mu = \frac{B\sigma_{yy}}{2\dot{E}}, \tag{3.3}$$

where B is a constant and $\dot{E}$ is the second invariant of the strain rate tensor.

(b) *The two-dimensional case*

Figure 1 shows a selection of numerical experiments in a vertical plane. In each of the four diagrams, contours of the extensional strain rate, $\dot{\epsilon}_{xx}$, are scaled relative to the maximum strain rate. The left-hand boundary is an axis of symmetry

Table 1. *Principal parameters used in numerical experiments*

	lithospheric mantle rheology	
Q_m	activation energy	500 kJ mol^{-1}
n	stress exponent	3
A_m	pre-exponential constant	10^{-13} Pa^{-3} s^{-1}
	simplified (weak) crustal rheology	
Q_c	activation energy	0 kJ mol^{-1}
n	stress exponent	3
A_c	pre-exponential constant	10^{-35} Pa^{-3} s^{-1}
	brittle–plastic crustal rheology	
Q_c	activation energy	300 kJ mol^{-1}
n	stress exponent	3
A_c	pre-exponential constant	10^{-16} Pa^{-3} s^{-1}
B	brittle stress constant	0.25
	other parameters	
L_o	initial lithospheric thickness	120 km
c_o	initial crustal thickness	33 km
ρ_c	crustal density	2850 kg m^{-3}
ρ_a	asthenosphere density	3185 kg m^{-3}
ρ_w	water density	1000 kg m^{-3}
α	coefficient of thermal expansion	3×10^{-5} K^{-1}
g	gravitational acceleration	9.81 m s^{-2}
R	universal gas constant	8.314 J mol^{-1} K^{-1}
T_m	initial Moho temperature	580 °C
T_a	asthenosphere temperature	1330 °C
k_c	thermal conductivity of crust	2.5 W m^{-1} K^{-1}
k_m	thermal conductivity of mantle	3.0 W m^{-1} K^{-1}
k_w	thermal conductivity of water	0.8 W m^{-1} K^{-1}
c_p	specific heat capacity	1000 m^2 s^{-2} K^{-1}
H_c	crustal heat production	1.1 μm W m^{-3}

and extension is driven by a constant force applied to the right-hand boundary. A temperature of 1330 °C is maintained at a depth of 120 km and buoyancy forces are included. Parameters for each experiment are given in the figure caption and in table 1.

Figure 1*a* shows strain rates as extension begins. Despite the strong depth dependence of viscosity, strain rate is approximately independent of depth. Deformation is concentrated near the left-hand boundary because the crust there is 2 km thicker, making the uppermost mantle hotter and weaker. Figure 1*b* shows the same experiment after extension has been in progress for 40 Ma. Strain rate is still independent of depth but the highest strain rate is now *ca.* 200 km away from the left-hand boundary. The maximum strain rate is much lower than in figure 1*a*.

Figure 1*c* is an example where strain rates do vary with depth as soon as extension

begins. The rheological parameters are the same as in figure 1*a* except that the plastic rheology in the crust has a higher value of A_c, making the crust weaker. The thick crust and high Moho temperature still concentrate extension in the lithospheric mantle near the left-hand boundary. Deformation in the crust is spread over a wider region because there is no initial weakness of the crust near the left-hand boundary, and, in contrast to figure 1*a*, the lower crust is weak enough to allow a decoupling of deformation. As deformation proceeds, the Moho rises very little in the region where the lithospheric mantle has its highest strain rate. Thus there is very little strengthening of the mantle in that region, and there is no reason why extension should slow down or stop until the driving force is removed.

Figure 1*d* also shows an example where strain rate varies with depth. The rheology is the same as in figure 1*c* but the initial weakness on the left-hand side is caused by higher than normal radioactive heat production in the crust. Both crust and lithospheric mantle are hotter and weaker and deformation is initially concentrated near the left-hand boundary in both layers. Thirty million years later, as in figure 1*d*, cooling of the uppermost lithospheric mantle means that the maximum strain rate in the mantle is *ca.* 400 km away from the left-hand boundary. The weakest part of the crust is only 350 km away from the boundary and the weak lower crust allows a pattern of offset deformation to occur.

A full analysis of extension in two dimensions is beyond the scope of this paper, but for the purpose of analysing our subsidence data, figure 1 makes some important points. When extension follows the pattern of figure 1*a*, *b*, each column of lithosphere has a strain rate governed by its own depth-integrated viscosity. Such cases can be analysed with a one-dimensional model, and such an analysis will also be compatible with the strain rate inversion which assumes that strain is independent of depth. If initial strain rates are more like figure 1*c*, a one-dimensional model is not sufficient and the strain rate inversion itself would be demonstrably invalid (White 1994). As cooling of the lithospheric mantle is not likely to slow extension in such cases, the deformation would be force-controlled anyway. Finally, cases such as figure 1*d* only start to display depth-dependent strain rates after most of the strain has accumulated: errors introduced by assuming pure shear are small, especially where the stretching factors are highest. A one-dimensional model is thus a useful approximation for numerical modelling of extension.

(*c*) *The one-dimensional case*

For the following calculations, we have adapted our finite-element model so that strain rate cannot vary with depth. This restriction is achieved by making the viscosity for non-pure-shear deformation artificially high.

Figure 2*a* shows the variation of strain rate with time for a very simple rheology. The crust has a very low viscosity that does not depend on temperature, while the lithospheric mantle is characterized by power-law creep. This rheology is probably not very realistic, but it does include the temperature dependence of viscosity in the lithospheric mantle. It is therefore useful for studying the fundamentals of strain rate variation without any complications from the effects of the crust. Once we have established these fundamentals, we will introduce more sophisticated rheologies.

Each example in figure 2*a* has a different magnitude of driving force and so the initial strain rate is different. For case (i), the initial strain rate is high and complete

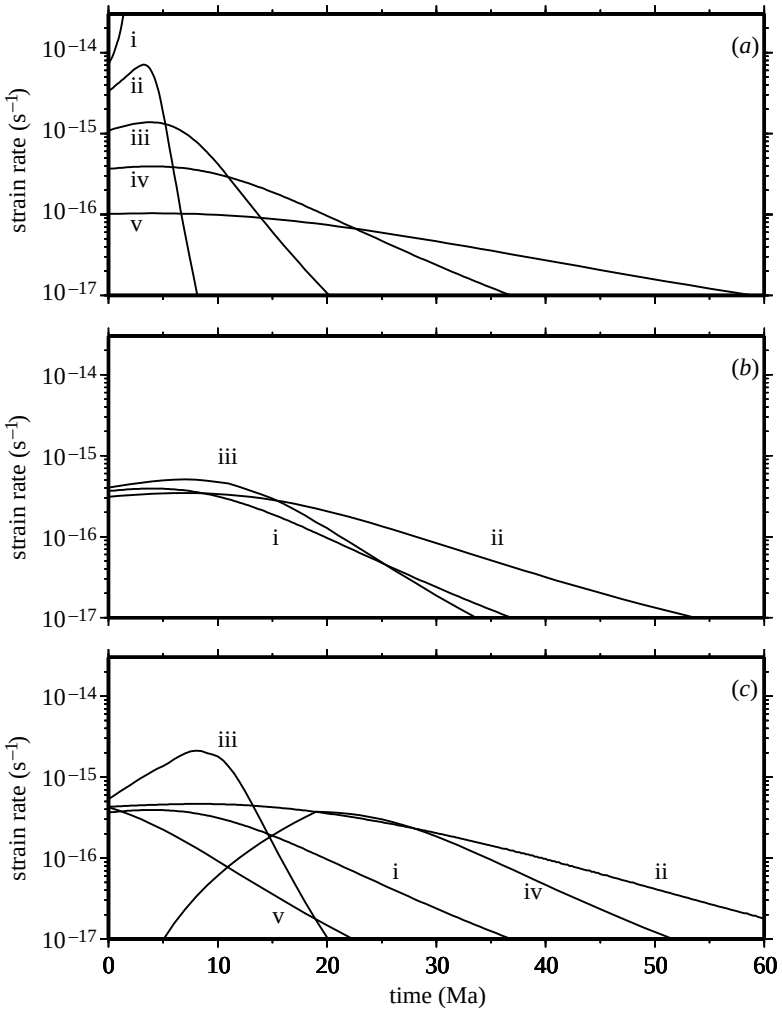

Figure 2. Variation of strain rate with time is plotted for a set of one-dimensional numerical experiments. (*a*) Each experiment has the same rheology (see table 1) but the driving force is different so that the initial strain rate varies. Higher initial strain rates yield shorter periods of extension. (*b*) Each experiment has a similar initial strain rate: (i) $Q_{\mathrm{m}} = 500$ kJ mol^{-1}, $n = 3$; (ii) $Q_{\mathrm{m}} = 300$ kJ mol^{-1}, $n = 3$; (iii) $Q_{\mathrm{m}} = 500$ kJ mol^{-1}, $n = 5$. (*c*) Each experiment has similar rheological parameters and a similar peak strain rate but the following differences: (i) same as figure 2*b*(i); (ii) sediments are included; (iii) brittle–plastic crustal rheology (table 1) is used; (iv) driving force increases linearly during the first 20 Ma of stretching; (v) an episode of stretching with $\beta = 1.2$ has occurred 30 Ma previously.

rifting of the lithosphere occurs before there is significant thermal diffusion. Strain rate increases with time because as extension proceeds, the same driving force acts on a progressively thinner lithosphere. In the other examples, strain rate initially rises for the same reason, but then mantle cooling becomes more important and strain rate is reduced. The time taken for the strain rate to become negligible (i.e. less than

$10^{-17}\,\mathrm{s}^{-1}$) is shorter for higher initial strain rates. If strain rate histories represent different locations in a basin, extension would continue longer where the stretching factor was lower (figure 1*a*, *b*).

A convenient way to compare numerical results with the results of our subsidence analysis is to plot maximum strain rate attained against total stretching factor. In figure 3*a*, the results from figure 2*a* have been summarized in this way. Each curve joins a set of experiments with the same rheological parameters but with a different magnitude of the driving force. In a real basin, an initial variation of strain rate with position might be caused by spatial variation of the driving force, by spatial variation of the viscosity, or by both. For instance, the driving force may vary with distance along the strike of a rift while the initial viscosity of the lithosphere varies perpendicular to the strike. In our experiments, curves obtained by the two types of variation are very similar and so this distinction is not important.

Changing the activation energy, Q_m, makes a considerable difference to the results (figure 3*a*). The sensitivity of viscosity to temperature changes is much greater when Q_m is high and so less cooling is needed to stop extension. Figure 3*b* shows the effect produced by changing the power-law exponent: a higher value of n leads to a higher stretching factor for a given strain rate. The strain rate history for $Q_\mathrm{m} = 500\,\mathrm{kJ\,mol}^{-1}$ with $n = 5$ (figure 2*b*) is much more like the $Q_\mathrm{m} = 500\,\mathrm{kJ\,mol}^{-1}$ with $n = 3$ case than the $Q_\mathrm{m} = 300\,\mathrm{kJ\,mol}^{-1}$ with $n = 3$ case. Thus, for small stretching factors, the value of Q_m rather than the ratio Q_m/n is a better guide to results.

The third rheological parameter, A_m, has little effect on the above relationships; changing A_m has a very similar effect to changing the driving force and simply moves points along the curves.

(*d*) *Analytical approximations*

In our model, most of the lithospheric strength lies just below the Moho so the variation in strain rate can be approximated by considering the evolution of the Moho temperature, T_m. For a power-law rheology, a temperature change of ΔT at the Moho lowers the strain rate from its initial value, $\dot{\epsilon}_\mathrm{o}$, to $\dot{\epsilon}_1$ where

$$\log_\mathrm{e}\dot{\epsilon}_\mathrm{o} - \log_\mathrm{e}\dot{\epsilon}_1 = \frac{Q_\mathrm{m}\Delta T}{RT_\mathrm{m}^2} - n\log_\mathrm{e}\beta. \tag{3.4}$$

In equation (3.4), we have assumed that the deviatoric stress is raised by a factor of β as the lithosphere thins. The temperature change required to lower the strain rate by an order of magnitude, ΔT_r, is therefore

$$\Delta T_\mathrm{r} = \{2.3 + n\log_\mathrm{e}\beta\}\frac{RT_\mathrm{m}^2}{Q_\mathrm{m}}, \tag{3.5}$$

which is *ca.* 34 °C when $Q_\mathrm{m} = 500\,\mathrm{kJ\,mol}^{-1}$, $T_\mathrm{m} = 580\,^\circ\mathrm{C}$ (853 K), and $\beta = 1.2$.

It is also possible to estimate how long it will take for the temperature to drop by this amount. Consider the temperature, T_s, which the Moho would have for a crustal thickness, c, if the geothermal gradient returned to its equilibrium condition. In our simplified model this temperature is

$$T_\mathrm{s} = \frac{H_\mathrm{c}c^2}{2k_\mathrm{c}} + \frac{k_\mathrm{m}\gamma_\mathrm{m}c}{k_\mathrm{c}}, \tag{3.6}$$

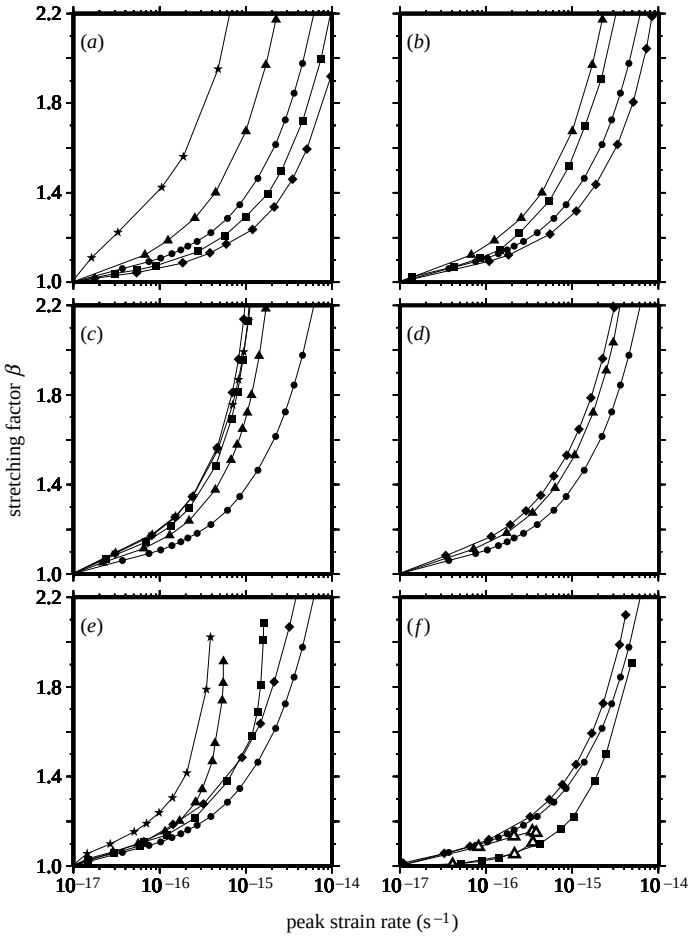

Figure 3. Total stretching factor is plotted against peak strain rate for one-dimensional numerical experiments. Each curve represents a set of experiments where the only parameter differing between experiments is the magnitude of the driving force. Experiment parameters are as in table 1, including the simplified crustal rheology, except where indicated. As a reference, the circles show the same experiments in each diagram. (*a*) Variation of activation energy. Stars: $Q_m = 100$ kJ mol^{-1}; triangles: $Q_m = 300$ kJ mol^{-1}; circles: $Q_m = 500$ kJ mol^{-1}; squares: $Q_m = 800$ kJ mol^{-1}; diamonds: $Q_m = 1200$ kJ mol^{-1}. (*b*) Variation of the power-law exponent. Triangles: $Q_m = 300$ kJ mol^{-1}, $n = 3$; squares: $Q_m = 500$ kJ mol^{-1}, $n = 5$; diamonds: $Q_m = 500$ kJ mol^{-1}, $n = 1$. (*c*) Effect of sediment blanketing. Diamonds: $\phi_o = 0.5$, $\lambda = 2$ km; stars: $\phi_o = 0.5$, $\lambda = 5$ km; squares: $\phi_o = 0.5$, $\lambda = 2$ km but $k_s = 0.8k_c$; triangles: $\phi_o = 0.5$, $\lambda = 2$ km but $k_s = 1.0k_c$. (*d*) Effect of a strong crust. Triangles: $A_c = 10^{-40}$ Pa^{-3} s^{-1}; diamonds: $A_c = 10^{-41}$ Pa^{-3} s^{-1}. (*e*) Effect of brittle deformation. Brittle–plastic crustal rheology of table 1 is used and initial Moho temperature is varied between experiments (560–655 °C) rather than driving force. Diamonds: brittle in crust only; squares: brittle in mantle and crust; triangles: brittle in mantle and crust; stars: brittle in mantle and crust with sediments included ($\phi_o = 0.5$, $\lambda = 2$ km). (*f*) The effects of force variation and of earlier extension. Diamonds: the driving force increases linearly with time for the first 10 Ma; squares: a stretching event of $\beta = 1.2$ has occurred 30 Ma earlier; triangles: each experiment has the same driving force but experienced a different stretching factor in an event 30 Ma earlier.

where H_c is the rate of heat production in the crust, k_c and k_m are the conductivities of the crust and mantle, and γ_m is the thermal gradient in the lithospheric mantle. As a rough approximation, the temperature varies according to

$$\frac{dT}{dt} = -\frac{(T - T_s)}{t_d}, \tag{3.7}$$

where t_d (*ca.* 60 Ma) is the thermal time constant of the lithosphere (Carlslaw & Jaeger 1959, p. 100). Equation (3.7) can be integrated if we assume that the mean velocity of the Moho during the thermal diffusion is approximately $\dot{\epsilon}_o c_o$, and thus

$$T_s \approx T_o - \dot{\epsilon}_o c_o t \left(\frac{dT_s}{dc}\right)_{c=c_o}, \tag{3.8}$$

where T_o is the initial Moho temperature and t is the time elapsed since extension began. Integrating equation (3.7) and expanding the result for $t < t_d$ then gives

$$\Delta T = \frac{\dot{\epsilon}_o c_o t^2}{2t_d} \left(\frac{dT_s}{dc}\right)_{c=c_o}. \tag{3.9}$$

The values of ΔT_r from equation (3.5) and of T_s from equation (3.6) now enable the duration of the extension, t_r, to be estimated. For a set of experiments with the same rheological parameters, this duration decreases as $\dot{\epsilon}_o$ increases, exactly as the strain rate histories in figure 2*a* show. Similarly, ΔT_r and hence t_r increase if n is increased or if Q is decreased. For example, dT/dc in our model is *ca.* 25 °C km^{-1}, and so combining equations (3.5) and (3.9) predicts that if t_r is in units of Ma and $\dot{\epsilon}_o$ is in units of s^{-1},

$$t_r \approx 4 \times 10^{-7} (\dot{\epsilon}_o)^{-1/2}. \tag{3.10}$$

For an initial strain rate of 3×10^{-15} s^{-1}, t_r should be *ca.* 7 Ma and a strain rate of 3×10^{-16} s^{-1} should give $t_r \sim 23$ Ma. These estimates agree well with the results of figure 2*a*.

4. Complications

(*a*) *The effect of sediment*

The effective viscosity of sediment is small compared with the rest of the lithosphere and so its mechanical effect on strain rate can be ignored. Sediments do, however, play an important role in controlling temperature within the lithosphere by blanketing (McKenzie 1981; Lucazeau & Le Douaran 1985). The Moho cools more slowly than it does when there are no sediments, which leads to a longer rift duration and a higher stretching factor for a given strain rate. The size of the effect depends on both the thickness and the thermal conductivity, k_s, of the sediments; typically the duration is increased by a factor of up to about 2, which increases the final stretching factor by a similar amount (case (ii) of figure 2*c*). In extreme cases, blanketing can result in the Moho temperature rising instead of falling as extension proceeds, causing extension to accelerate rather than slow down.

The physical properties of sediments are hard to specify since they vary considerably with lithology and also with degree of compaction of the sediment (Sclater &

Christie 1980). We assume that the conductivity of typical sediment can be estimated using

$$k_{\mathrm{s}} = k_{\mathrm{c}}(1-\phi) + k_{\mathrm{w}}\phi, \tag{4.1}$$

where ϕ is the porosity and k_{w} is the conductivity of water. A similar expression is used to calculate sediment density. The porosity at a depth z is assumed to depend on a compaction depth λ,

$$\phi = \phi_{\mathrm{o}} \exp(z/\lambda). \tag{4.2}$$

Numerical results for different sediment parameters are shown in figure 3*c*. Experiments denoted by stars have a surface porosity of $\phi_{\mathrm{o}} = 0.5$ and a compaction length of 2 km. Increasing the compaction length to 5 km has little effect because the change in conductivity compensates for the change in density. Setting k_{s} to be constant rather than being depth dependent, which may be more appropriate for sandstones (Allen & Allen 1990), produces similar results if $k_{\mathrm{s}} = 0.8k_{\mathrm{c}}$. If k_{s} is equal to the crustal conductivity, however, the blanketing effect is reduced. In our calculations, we maintain isostatic balance with unextended lithosphere and we fill the basin completely with sediment at every time-step. If the top of the lithospheric column is initially above sea level, or if there is significant palaeobathymetry during basin formation, the effect of sediment blanketing is reduced.

Equations (3.5) and (3.9) in our analytical approximation are still valid. The influence of the sediment can be accounted for by adjusting T_{s},

$$T_{\mathrm{s}} = \tfrac{1}{2}H_{\mathrm{c}}\left(\frac{c^2}{k_{\mathrm{c}}} + \frac{2cs}{k_{\mathrm{s}}} + \frac{s^2}{k_{\mathrm{s}}}\right) + k_{\mathrm{m}}\gamma_{\mathrm{m}}\left(\frac{c}{k_{\mathrm{c}}} + \frac{s}{k_{\mathrm{s}}}\right), \tag{4.3}$$

which gives

$$T_{\mathrm{s}} \approx \tfrac{1}{2}k_{\mathrm{c}}H_{\mathrm{c}}\left(\frac{c}{k_{\mathrm{c}}} + \frac{s}{k_{\mathrm{s}}}\right)^2 + k_{\mathrm{m}}\gamma_{\mathrm{m}}\left(\frac{c}{k_{\mathrm{c}}} + \frac{s}{k_{\mathrm{s}}}\right). \tag{4.4}$$

The significance of sediment density is that s is inversely proportional to $(\rho_{\mathrm{a}} - \rho_{\mathrm{s}})$, so the combined influence of the sediment parameters on blanketing depends on the factor,

$$\frac{1}{k_{\mathrm{s}}(\rho_{\mathrm{a}} - \rho_{\mathrm{s}})}. \tag{4.5}$$

(*b*) *The influence of crust*

Although the viscosity of the crust is unlikely to play a significant role in stopping extension, it can be important in determining the strain rate during the early stages of extension. Figure 3*d* shows that an increased crustal viscosity (lower A_{c}) leads to a higher stretching factor for a given peak strain rate. It is still a decrease in Moho temperature that causes extension to stop, but the temperature change required (ΔT_{r}) is greater than in equation (3.5). The Moho temperature must decrease by a certain amount (say, 15 °C) before mantle viscosity equals crustal viscosity; then a further drop of *ca.* 30 °C is then required to stop extension. The result is a longer rift duration with a higher stretching factor.

A better approximation to crustal rheology permits either brittle or power-law creep deformation. The brittle rheology amplifies the initial rise in strain rates caused

by lithospheric thinning, especially if the crust is relatively strong (case (iii) of figure 2c). For a strong crust, the temperature at the brittle–plastic transition controls the strain rate during the early stages of deformation. As the crust is thinned, the brittle–plastic transition stays at a more or less constant depth, but its temperature increases and so strain rate increases until strengthening of the mantle becomes more important. The brittle crust affects both the peak strain rate and the final stretching factor reached, but the relationship between the two is very similar to our results for a simplified crustal rheology (compare the diamonds of figure 3*e* with those in figure 3*d*).

The crust may actually strengthen during extension if the lower crust is stronger than the upper crust. This situation arises if the reduction in strength caused by higher temperatures is outweighed by the crust being more mafic at depth: pyroxenes, for example, are stronger than feldspars at the same temperature (Kirby & Kronenburg 1987). A lower water content in the lower crust would also increase its strength. To control strain rate throughout extension, lower crust needs to be stronger than lithospheric mantle, and the stretching factor needs to be small enough to prevent the lower crust becoming brittle. Under these conditions, equations (3.5) and (3.9) still apply as long as the temperature and depth of the strongest part of the lower crust are used instead of T_{m} and c_{o}. The duration of stretching is slightly shorter for a given activation energy, so a lower crust with $Q_{\mathrm{c}} = 400\,\mathrm{kJ\,mol^{-1}}$ gives similar results to lithospheric mantle with $Q_{\mathrm{m}} = 500\,\mathrm{kJ\,mol^{-1}}$.

(*c*) *Brittle deformation in the mantle*

An important question is whether there is brittle deformation in the lithospheric mantle during extension and, if there is, whether it prevents the viscosity increasing enough to stop extension (Sawyer 1985; England 1986). During extension the Moho moves upwards and so, if Byerlee's law applies in the mantle as well as in the crust, brittle deformation will occur in the mantle once a certain stretching factor is reached. Once the uppermost mantle becomes brittle it no longer strengthens, but extension can still be limited by cooling because the base of the brittle zone rises as extension proceeds. Some dynamical models of extension (e.g. Braun & Beaumont 1987; Dunbar & Sawyer 1989) assume that the top of the lithospheric mantle is already brittle when extension begins, making it difficult to limit extension by cooling unless the strain rate is very small. An argument against such widespread brittle deformation is that there are few mantle earthquakes in regions of continental extension (Chen & Molnar 1983).

For our experiments, we assume that the value of B in equation (3.3) is the same in the mantle as in the crust. If the mantle is relatively dry, B may in fact be greater there. In figure 3*e* (squares), we show results when the lithospheric mantle becomes brittle during extension. When the strain rate exceeds about $10^{-15}\,\mathrm{s^{-1}}$ ($\beta > 1.6$), only a small increase in strain rate is required to produce a large change in stretching factor. For a slightly different rheology (figure 3*e*, triangles), the uppermost mantle is brittle as soon as deformation begins; stretching factors are very sensitive to strain rate for $\beta > 1.2$. A rheology with a substantial brittle zone in the mantle is therefore unlikely to produce basins of gently varying stretching factors unless $\beta < 1.2$.

When the effects of brittle deformation and sedimentation are combined, stretching factors for a given strain rate are raised still further (figure 3*e*, stars). The sediments

provide a moderating effect on the early increase in strain rates because their weight increases the stress required for brittle deformation in the underlying lithosphere.

Strengthening of the lithosphere may be limited by means other than brittle deformation, such as semibrittle behaviour (Kohlstedt *et al.* 1995) and high-stress plasticity (Goetze 1978). In each case, the deviatoric stress that can be supported in the upper mantle is limited, so the effect on our model is similar to that of Byerlee's law: the final stretching factor depends very sensitively on the strain rate once the limiting stress is reached.

(*d*) *Variation in driving forces*

So far, we have assumed that the driving force remains constant during extension. In practice, it is bound to vary to some extent. Buoyancy forces, although they may be small compared with the driving force, must change as the crustal thickness changes. It is also unrealistic to assume that the driving force reaches a maximum instantaneously.

For a given rheology, any decrease in the driving force during extension produces a stretching factor below that predicted in figure 3. An increasing driving force gives a higher stretching factor for a given peak strain rate, but the difference is small. The results in figure 3*f* (diamonds) are for a force that increases linearly from zero to a maximum over 10 Ma and then remains at that maximum. Their closeness to the results for a constant force is useful because, when we analyse extension in real basins, differences in the growth of driving forces do not obscure similarities in rheology. Case (iv) of figure 2*c* shows the time dependence of strain rate when the driving force rises to a maximum over a period of 20 Ma. The strain rate is negligible for the first few million years and reaches a maximum at the same time as the force.

(*e*) *Prior stretching events*

Many sedimentary basins have had more than one period of extension. In our model, secondary events can be generated by increasing the driving force some time after the first stretching event has ended. The increase in force required to produce significant secondary extension depends on the stretching factor for the first event and on the time-interval between events, and is reduced if there is significant sediment blanketing or if the power-law exponent is greater than 3. For the experiments discussed here, we increase the magnitude of the force by factors of 1.2–5.0.

The existence of an earlier stretching event has a marked influence on later strain rate variation, especially if the two rifting episodes are separated by less than 60 Ma. Case (v) of figure 2*c* shows the strain rate history during a second event when an extension of $\beta = 1.2$ occurred 30 Ma earlier. Strain rate begins to fall as soon as extension starts and the duration of rifting is much less than for a first event of similar maximum strain rate (compare with case (i)). The reason for the comparatively rapid drop in strain rates is that a temperature perturbation from the equilibrium geotherm, θ, is inherited from the first rift event. The larger the first event, and the shorter the separation between events, the larger the inherited perturbation.

In our analytical approximation, there is an additional term in equation (3.9) related to the decay of this perturbation,

$$\Delta T = \frac{\dot{\epsilon}_{\mathrm{o}} c_1 t^2}{2t_{\mathrm{d}}} \frac{\mathrm{d}T_{\mathrm{s}}}{\mathrm{d}c} + \theta \frac{t}{t_{\mathrm{d}}}, \tag{4.6}$$

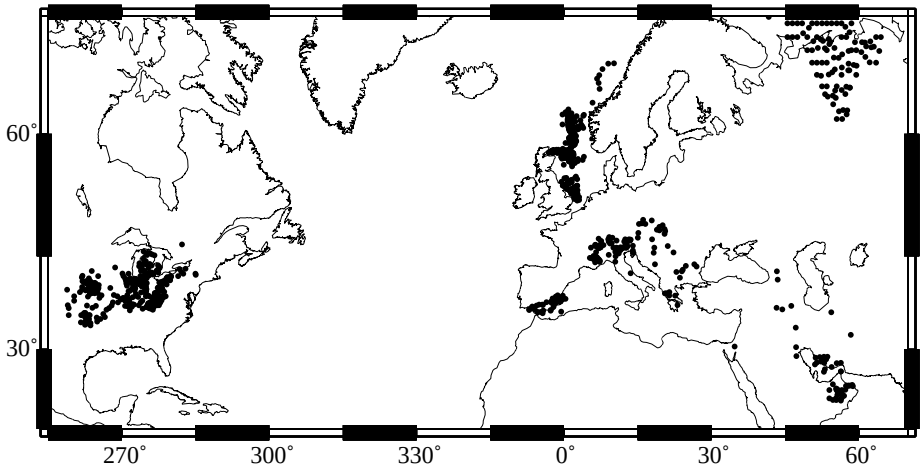

Figure 4. Mercator projection showing locations of stratigraphic sections, which were derived from field logging, industry wells and seismic reflection data. Regions were chosen to include continuous, shallow-water, marine sections from different portions of the geological time-scale. Palaeowater depths are generally well constrained and syn-rift topography has wavelengths of *ca.* 20 km with small amplitudes so that the flexural rigidity of the lithosphere can be ignored.

where c_1 is the crustal thickness when the second event starts. The duration of the second event is therefore

$$t_\mathrm{r} = \frac{1}{c_1 \dot{\epsilon}_\mathrm{o}} \left(\frac{\mathrm{d}T_\mathrm{s}}{\mathrm{d}c} \right)^{-1} \left\{ -\theta + \left(\theta^2 + 2c_1 \dot{\epsilon}_\mathrm{o} t_\mathrm{d} \Delta T_\mathrm{r} \frac{\mathrm{d}T_\mathrm{s}}{\mathrm{d}c} \right)^{1/2} \right\} \tag{4.7}$$

and decreases as θ increases.

Figure 3*f* includes results from two sets of experiments that incorporate a prior rifting event. In one set (squares), a rifting event with $\beta = 1.2$ has occurred 30 Ma before the event that is plotted. The inherited temperature perturbation is therefore the same in each experiment. The stretching factors for a given strain rate are considerably lower than for single events, particularly at strain rates of *ca.* $10^{-15}\ \mathrm{s}^{-1}$.

The other set of results (triangles) form a distinctive curve. The experiments have different values of β for the first event, and may be more appropriate for comparison with real basins, where the sizes of first events may vary as much as later events. The driving force is the same for each experiment but the initial crustal thickness differs, so the initial viscosity and subsequent strain rate histories are different. When the viscosity is initially large, neither event produces much strain. When the viscosity is initially small, the first event is large but the Moho cools so much that the second event is very small. The largest second event occurs when both events have stretching factors of *ca.* $\beta = 1.1$, and strain rates of more than $4 \times 10^{-16}\ \mathrm{s}^{-1}$ are not found in second events.

5. Inversion of subsidence data

To determine strain rate histories, we and our colleagues have collated and digitized over 2000 stratigraphic sections from extensional sedimentary basins (figure 4). These

data span the past 600 Ma and are from regions where stratigraphic sequences are as complete as possible. The lack of deeply penetrating boreholes means that data from highly extended portions of continental margins are lacking. Tectonic subsidence has been calculated and modelled using an inversion algorithm to determine temporal strain rate variation. A small sample of our data-set is shown in figure 5. Inversion yields excellent fits between theoretical and observed subsidence, and strain rate profiles are generally consistent with independent geological information about the duration and number of rift periods.

Our data-set can be used to place constraints upon the equilibrium thickness of the continental lithosphere, at least in regions with Phanerozoic sedimentary cover. Figure 6 shows how the misfit between theoretical and observed subsidence depends on three parameters used in our inversion. The smallest misfit is obtained when the lithospheric thickness is 120 km, the asthenospheric temperature is 1400 °C and the thermal expansion coefficient is $3.3 \times 10^{-5}\ ^{\circ}\mathrm{C}^{-1}$. There is a trade-off in the effects of asthenospheric temperature and thermal expansion coefficient, but there are independent constraints on both those parameters. The misfit function therefore demonstrates that the lithospheric thickness must be 120 ± 15 km and that the asthenospheric temperature is $1400 \pm 150\ ^{\circ}\mathrm{C}^{-1}$.

6. Discussion

(*a*) *Evidence for viscosity-controlled extension*

Peak strain rates from our subsidence inversions are plotted against stretching factor in figure 7 and compared with our numerical modelling in figure 8. A rifting episode is assumed to have ceased if the strain rate falls below $10^{-17}\ \mathrm{s}^{-1}$. There are often several episodes of extension within a basin and each of these events has been plotted as a separate point.

In each basin, peak strain rates are less than $2 \times 10^{-15}\ \mathrm{s}^{-1}$ and there is a smooth distribution of data points rather than a concentration at a single strain rate or stretching factor. Extension is therefore slow enough for appreciable thermal diffusion to occur. Variations in strain rate of two orders of magnitude between places only tens of kilometres apart are easily explained by a strong temperature dependence of viscosity.

A correlation between peak strain rate and final stretching factor is seen in each of the basins. The form of the correlation is similar to that obtained for viscosity-controlled extension (figure 3), although we do not have data for stretching factors above *ca.* 1.5. It is significant that the relationship of stretching factor to strain rate is much the same in each basin. For viscosity-controlled extension, differences in the magnitude of the driving forces between basins do not affect this relationship, only parameters such as Q_{m} that might well be the same in each case.

When there are two or more episodes of rifting, our modelling predicts that for a given peak strain rate, the later events should have a lower stretching factor than the first event. A comparison of figure 8*a* with 8*b* shows that secondary events do tend to have lower stretching factors. Data points are only plotted in figure 8*b* when a prior event is detected in the inverted subsidence curve, although there may be undetected earlier events in other wells.

If the lithosphere is stronger after it has been stretched, a large rift event should make it relatively difficult to stretch the lithosphere a second time. Large first events

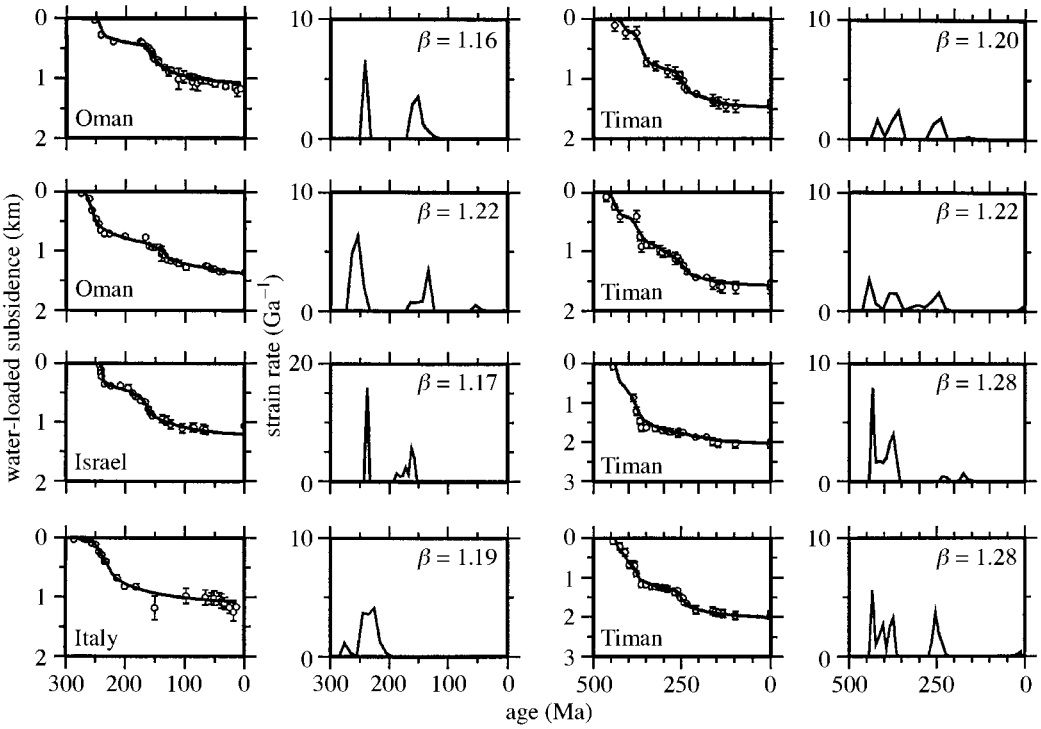

Figure 5. Strain rate inversion of 16 stratigraphic sections which illustrate the variety of subsidence data used. Left-hand panels: circles, tectonic (i.e. water-loaded) subsidence data produced by standard decompaction and backstripping; vertical bars, $2\sigma_i$; solid line, best-fitting theoretical subsidence curve. Right-hand panels: linearly interpolated strain rate distribution obtained by inversion and corresponding to best-fitting subsidence curve. No *a priori* information about the duration of rifting, the number of rift episodes, or the total stretching factor has been used. Error analysis demonstrates that strain rate peaks are resolved to better than a factor of two (95% confidence level; White 1994), reflecting structure within the observed subsidence data. Multiply by 3.17×10^{-17} to convert units from Ga^{-1} to s^{-1}.

should be associated with relatively small second events, and large second events with relatively small first events. Figure 9 shows that, in the North Sea, the stretching factors for successive events are related in this manner. A similar pattern is found in the other basins.

(*b*) *Evidence against force-controlled extension*

There are circumstances under which force-controlled extension might also give a correlation between total stretching factor and peak strain rate. An example is if a driving force acts for 20 Ma throughout a basin and the strain rate in each part of the basin remains constant during that time. For the correlation to be the same in every basin, however, the rift duration would have to be the same in each case. It seems unlikely that driving forces in different basins always act for the same length of time.

If viscosity does not increase during extension, places that have relatively high strain rates during a second stretching event should be the same as those that had

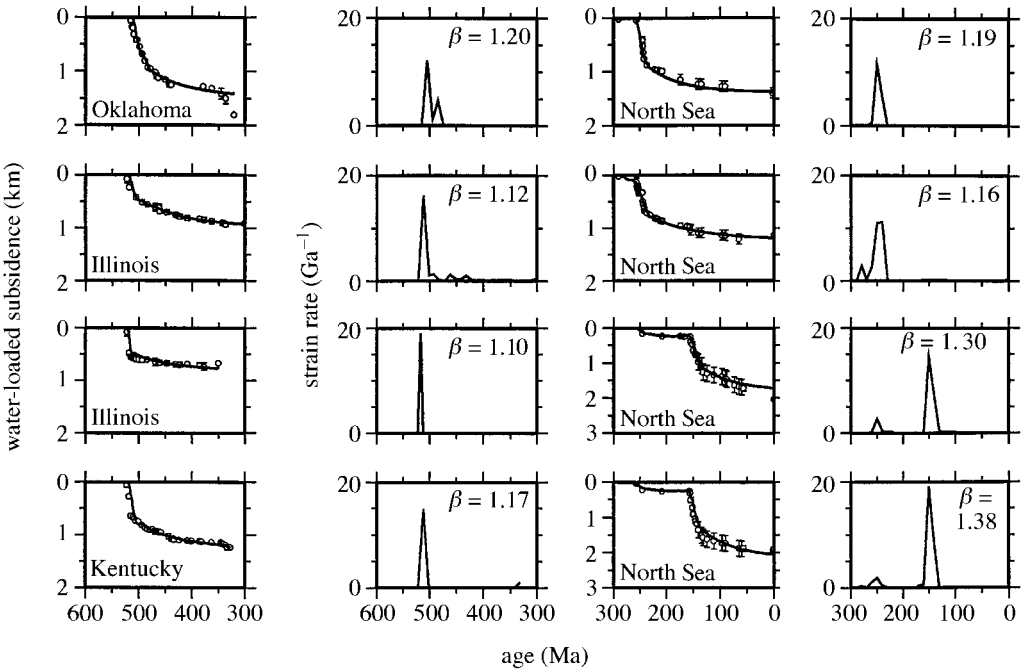

Figure 5. (*Cont.*)

high strain rates in the first event. Force-controlled extension should therefore give a positive correlation between stretching factors for the first and second events. This is not the case in any basin we have studied. In fact the opposite is true, as figure 9 shows for the North Sea. Figure 8*b* shows that secondary events have smaller stretching factors for a given strain rate, and therefore shorter rift durations. There is no reason this should be the case if force variations control the strain rate.

Using equation (2.1), we showed that the action of buoyancy forces does not lead to a relationship between strain rate and stretching factor that is the same in every basin, whether those buoyancy forces are driving extension or opposing it. There is no sign in the data of different parts of a basin reaching the same stretching factor, or final crustal thickness, regardless of the strain rate. Hence it is unlikely that buoyancy forces play a dominant role in halting extension. The driving force must, therefore, be significantly greater in magnitude than any opposing buoyancy forces.

Our data do not rule out the possibility that buoyancy forces are driving extension, but they indicate that in those circumstances it is still the change in viscosity caused by cooling of the lithospheric mantle that controls the strain rate. This behaviour is compatible with the dependence of strain rate on viscosity proposed by Jones *et al*. (1996) in the western United States. The basins we have studied, however, are marine for most if not all of their histories, and so it is unlikely they had thick or elevated crust during extension.

(*c*) *Estimating the lithospheric rheology*

The rheological constant that most affects the relationship between stretching factor and strain rate is Q_{m}, the activation energy. The power-law exponent n has a

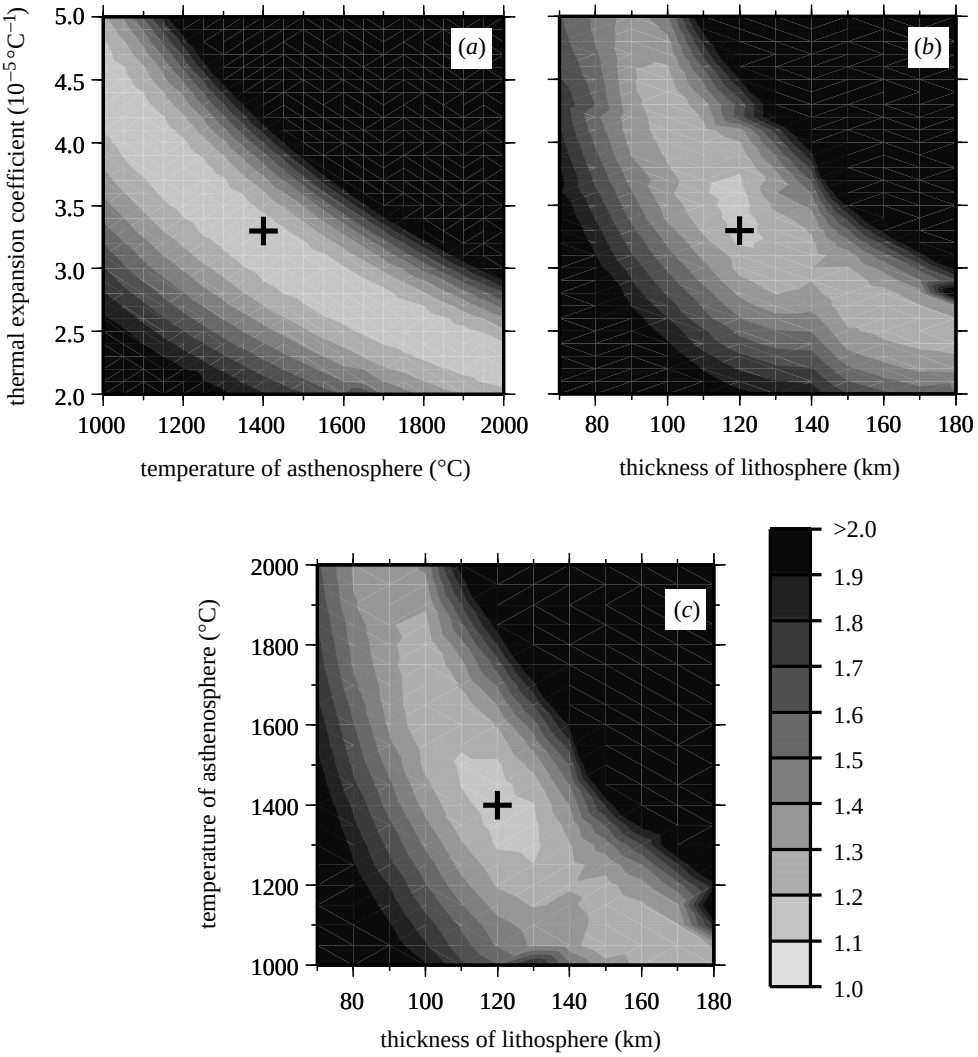

Figure 6. Misfit, χ^2, between theoretical and observed subsidence for a set of nine wells from the southern North Sea (Jarvis 1995). Misfit function is calculated for a range of values of equilibrium lithospheric thickness, asthenospheric temperature, and thermal expansion coefficient. The trade-off with strain rate was circumvented by constraining the rifting period using independent observations. Minimum misfit was found by inversion and occurs at a point indicated by the three black crosses (120 ± 15 km, 1400 ± 150 °C, $3.3 \pm 0.3 \times 10^{-5}$ °C^{-1}). (*a*) Slice through contoured misfit function for a lithospheric thickness of 125 km. (*b*) Slice orthogonal to (*a*) for asthenosphere temperature of 1333 °C. (*c*) Slice orthogonal to (*b*) and (*c*) for thermal expansion coefficient of 3.28×10^{-5} °C^{-1}. We have obtained similar results for North American data.

relatively small effect at $\beta < 1.5$ and the pre-exponential constant, A_{m}, has no effect (although both n and A_{m} affect initial strain rate). In figure 8*a*, we compare all strain rate data with our numerical results for a weak crustal rheology. An activation energy of $Q_{\mathrm{m}} = 500$ kJ mol^{-1} gives a reasonable fit at high strain rates but the data plots

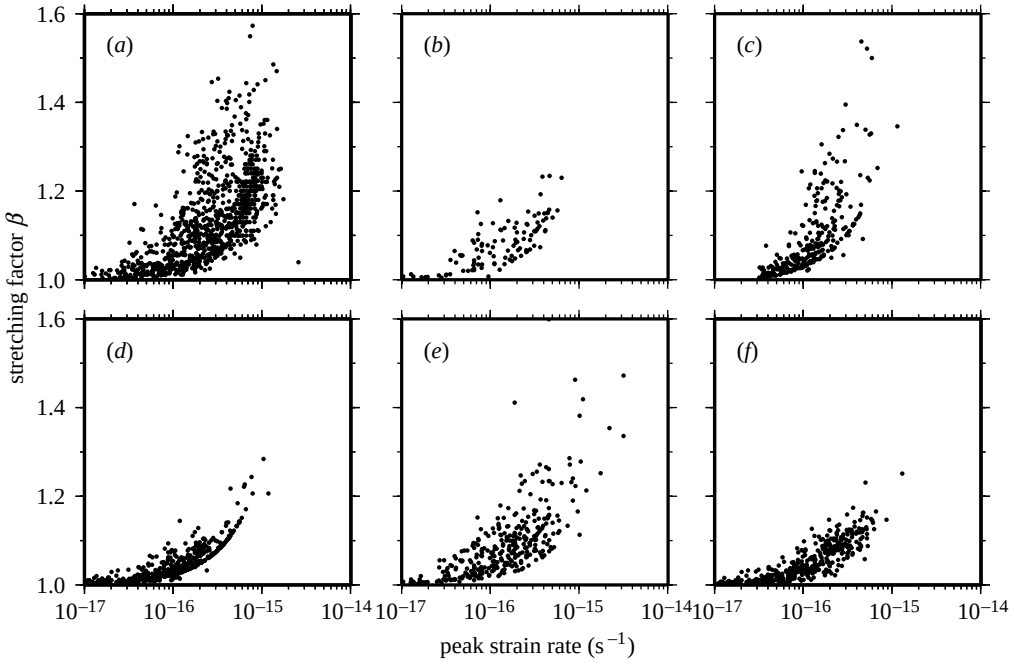

Figure 7. Results of strain rate inversion plotted region by region. Stretching events are treated as finished when the strain rate has dropped below 10^{-17} s^{-1} except for (*c*), where 3×10^{-16} s^{-1} is used. Strain rates have errors of a factor of two, stretching factors have errors of about 0.05. Many wells show multiple episodes of stretching, each of which is included in (*a*)–(*e*) with its own stretching factor and peak strain rate. Secondary events are also plotted separately in (*f*), except for Timan–Pechora, where an interval of *ca.* 200 Ma allows thermal perturbation to decay between events.

below the theoretical curve at low strain rates. A much higher activation energy ($Q_\mathrm{m} = 1200$ kJ mol^{-1}) provides a better fit at low strain rates but is less satisfactory at strain rates around 10^{-15} s^{-1}. Since a value of $Q_\mathrm{m} \sim 500$ kJ mol^{-1} agrees with the results of laboratory experiments on dry olivine, and since it is unlikely that common mantle minerals have much higher activation energies (Kirby & Kronenburg 1987), we consider this value to be representative of the rheology of the lithospheric mantle.

The curves plotted in figure 8*a* are for our simplest model, but alternative fits to the data can be obtained by combining the effects of the various complicating factors we have examined. Many of the data points with low strain rates are second or third rift events, so one would expect them to have a lower stretching factor than the curves predicted by our simplest models. When the peak strain rate is less than 10^{-16} s^{-1}, the duration of extension required before strain rates fall below 10^{-17} s^{-1} is more than 60 Ma (figure 2*a*). At low strain rates, therefore, it is more likely that the driving force is removed before extension is stopped by cooling of the mantle. In such circumstances, our theoretical curve indicates the maximum stretching factor possible for a given strain rate.

There is no sign in our data of the effects of brittle deformation in the mantle (figure 3*e*). We do find strain rates above 10^{-15} s^{-1}, and the data are distributed

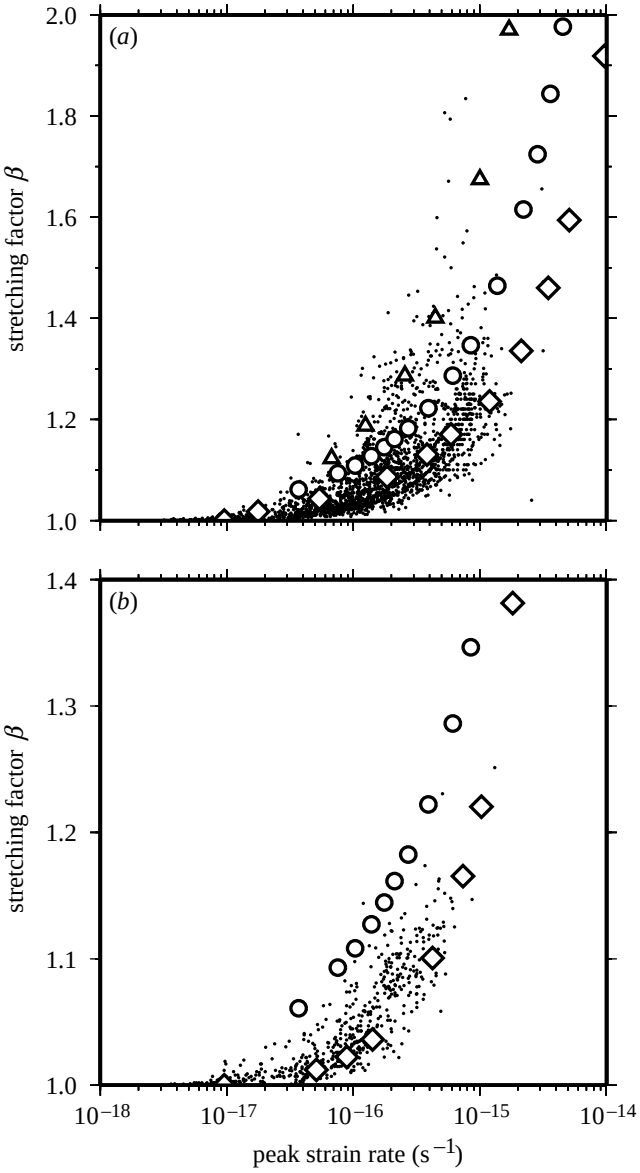

Figure 8. (*a*) Small dots, inverted strain rate data for 2195 separate rifting episodes. Large symbols, model results from figure 3*a*: triangles, $Q_m = 300$ kJ mol^{-1}; circles, $Q_m = 500$ kJ mol^{-1}; diamonds, $Q_m = 1200$ kJ mol^{-1}. (*b*) Small dots, data for secondary rift events from figure 7*f*. Large symbols, model results including effects of previous rifting: circles, as in (*a*) with no prior rifting; diamonds, $Q_m = 500$ kJ mol^{-1} with rift event of $\beta = 1.2$ occurring 30 Ma before the event shown.

smoothly. The absence of stretching factors above 1.4 is due to the type of basins we have studied, but it is possible that at higher stretching factors the relationship between strain rate and stretching factor changes, as in the experiments shown by

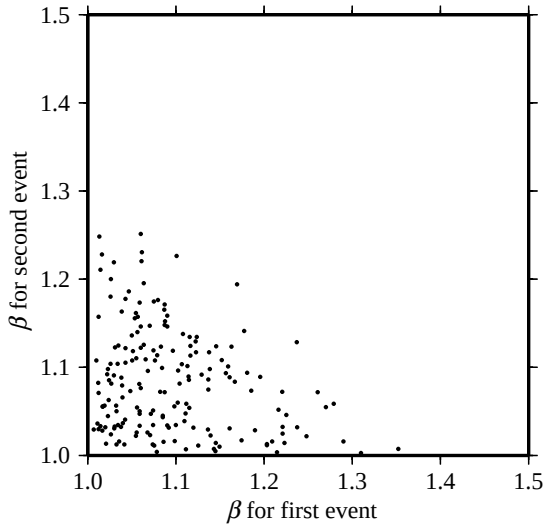

Figure 9. Stretching factors for first and second events in the North Sea. Cooling and strengthening of the lithosphere makes the second event small where the first event is large.

squares in figure 3*e*. Our results do provide evidence against there being an extensive zone of brittle deformation in the mantle when extension begins. If such a zone were present, it would be difficult to stop extension at strain rates above *ca.* 3×10^{-16} s^{-1} (cf. triangles in figure 3*e*). A brittle zone in the mantle is an important feature of many previous dynamical models of extension (e.g. Braun & Beaumont 1987; Dunbar & Sawyer 1989; Buck 1991). Its absence indicates that, compared with those models, either (i) the Moho temperature is hotter; (ii) the rheological constant, A_m, is higher; or (iii) the stress required for brittle failure in the mantle is higher. We have not attempted to constrain A_m, the Moho temperature, or the magnitude of the driving force, because the effects of these three parameters are hard to separate.

Sediment blanketing and the strength of the crust are probably responsible for some scatter in our data. Sediment lithology, for example, varies considerably between basins and the composition of the crust may vary significantly as well. Some scatter will be caused by inaccuracies in subsidence curves and in their inversion. Faulting of the upper crust means the lithosphere is not a perfect continuum, and extension will not occur by perfectly pure shear, but it is encouraging that data from different basins appear to tell a consistent story.

The errors introduced by our assumptions should be easier to quantify when we analyse the spatial distribution of strain rate within each basin. The influence of nearby faults can be assessed and a two-dimensional method used to improve the accuracy of subsidence inversion. Construction of strain rate profiles will allow comparison with dynamical models in a vertical plane (such as figure 1). Further constraints can then be placed on the rheology by requiring it to approximate pure shear throughout extension.

A. Butler, B. Hall, D. Hanne, E. Jarvis, N. O'Leary, C. Trowell, J. Turner and D. Wooler generously allowed us to use their data. We are grateful to P. Bellingham, S. Jones and P. Wheeler for their comments and to N. J. Kusznir and A. B. Watts for helpful reviews.

References

Allen, P. A. & Allen, J. R. 1990 *Basin analysis*. Oxford: Blackwell Scientific Publications.

Artyushkov, E. V. 1973 Stresses in the lithosphere caused by crustal thickness inhomogeneities. *J. Geophys. Res.* **78**, 7675–7708.

Barton, P. & Wood, R. 1984 Tectonic evolution of the North Sea basin: crustal stretching and subsidence. *Geophys. J. R. Astr. Soc.* **79**, 987–1022.

Bassi, G. 1991 Factors controlling the style of continental rifting: insights from numerical examples. *Earth Planet. Sci. Lett.* **105**, 430–452.

Bassi, G. 1995 Relative importance of strain rate and rheology for the mode of continental extension. *Geophys. J. Int.* **122** 195–210.

Bassi, G., Keen, C. E. & Potter, P. 1993 Contrasting styles of rifting: models and examples from the eastern Canadian margin. *Tectonics* **12**, 639–655.

Bennett, R. A., Rodi, W. & Reilinger, R. E. 1996 Global Positioning System constraints on fault slip rates in southern California and northern Baja, Mexico. *J. Geophys. Res.* **101**, 21 943–21 960.

Billiris, H. (and 13 others) 1991 Geodetic determination of tectonic deformation in central Greece from 1900 to 1988. *Nature* **350**, 124–129.

Bott, M. H. P. & Kusznir, N. J. 1979 Stress distributions associated with compensated plateau uplift structures with application to the continental splitting mechanism. *Geophys. J. R. Astr. Soc.* **56**, 451–459.

Brace, W. F. & Kohlstedt, D. L. 1980 Limits on lithospheric stress imposed by laboratory experiments. *J. Geophys. Res.* **85**, 6248–6252.

Braun, J. & Beaumont, C. 1987 Styles of continental rifting: results from dynamic models of lithospheric extension. In *Sedimentary basins and basin-forming mechanisms* (ed. C. Beaumont & A. J. Tankard). *Can. Soc. Petrol. Geol. Mem.* **12**, 241–258.

Buck, W. R. 1991 Modes of continental lithospheric extension. *J. Geophys. Res.* **96**, 20 161–20 178.

Byerlee, J. D. 1968 Brittle–ductile transition in rocks. *J. Geophys. Res.* **73**, 4741–4750.

Carlslaw, H. S. & Jaeger, J. C. 1959 *Conduction of heat in solids*, 2nd edn. Oxford University Press.

Chen, W. P. & Molnar, P. 1983 The depth distribution of intracontinental and intraplate earthquakes and its implications for the thermal and mechanical properties of the lithosphere. *J. Geophys. Res.* **88**, 4183–4214.

Christensen, U. R. 1992 An Eulerian technique for thermomechanical modelling of lithospheric extension. *J. Geophys. Res.* **97**, 2015–2036.

Dunbar, J. A. & Sawyer, D. S. 1989 How preexisting weaknesses control the style of continental breakup. *J. Geophys. Res.* **94**, 7278–7792.

England, P. C. 1983 Constraints on extension of continental lithosphere. *J. Geophys. Res.* **88**, 1145–1152.

England, P. C. 1986 Comment on 'Brittle failure in the upper mantle during extension of continental lithosphere' by Dale S. Sawyer. *J. Geophys. Res.* **91**, 10 487–10 490.

Frohlich, C. 1989 The nature of deep focus earthquakes. *A. Rev. Earth Planet. Sci.* **17**, 227–254.

Goetze, C. 1978 The mechanisms of creep in olivine. *Phil. Trans. R. Soc. Lond.* A **288**, 99–119.

Hellinger, S. J. & Sclater, J. G. 1983 Some comments on two-layer extensional models for the evolution of sedimentary basins. *J. Geophys. Res.* **88**, 8251–8270.

Hirth, G. & Tullis, J. 1994 The brittle–plastic transition in experimentally deformed quartz aggregates. *J. Geophys. Res.* **99**, 11 731–11 747.

Houseman, G. A. & England, P. C. 1986 A dynamical model of lithospheric extension and sedimentary basin formation. *J. Geophys. Res.* **91**, 719–729.

Jackson, J., Haines, J. & Holt, W. 1992 The horizontal velocity field in the deforming Aegean Sea region determined from the moment tensors of earthquakes. *J. Geophys. Res.* **97**, 17 657–17 684.

Jackson, J., Haines, J. & Holt, W. 1994 A comparison of satellite laser ranging and seismicity data in the Aegean region. *Geophys. Res. Lett.* **21**, 2849–2852.

Jarvis, E. L. 1995 Quantification of Permo–Triassic lithospheric stretching, southern North Sea. PhD thesis, University of Cambridge, UK.

Jarvis, G. T. & McKenzie, D. P. 1980 Sedimentary basin formation with finite extension rates. *Earth Planet. Sci. Lett.* **48**, 42–52.

Jones, C. H., Unruh, J. R. & Sonder, L. J. 1996 The role of gravitational potential energy in active deformation in the southwestern United States. *Nature* **381**, 37–41.

Keen, C. E. 1985 The dynamics of rifting: deformation of the lithosphere by active and passive driving forces. *Geophys. J. R. Astr. Soc.* **80**, 95–120.

Kirby, S. H. & Kronenburg, A. K. 1987 Rheology of the lithosphere: selected topics. *Rev. Geophys.* **25**, 1219–1244.

Kohlstedt, D. L., Evans, B. & Mackwell, S. J. 1995 Strength of the lithosphere: constraints imposed by laboratory experiments. *J. Geophys. Res.* **100**, 17 587–17 602.

Kusznir, N. J. & Park, R. G. 1987 The extensional strength of the continental lithosphere, its dependence on geothermal gradient, and crustal composition and thickness. In *Continental extensional tectonics* (ed. M. P. Coward, J. F. Dewey & P. L. Hancock). *Geol. Soc. Lond.* (Spec. Publ.) **28**, 35–52.

Lucazeau, F. & Le Douaran, S. 1985 The blanketing effect of sediments in basins formed by extension: a numerical model. Application to the Gulf of Lion and Viking graben. *Earth Planet. Sci. Lett.* **74**, 92–102.

McKenzie, D. 1978 Some remarks on the development of sedimentary basins. *Earth Planet. Sci. Lett.* **40**, 25–32.

McKenzie, D. 1981 The variation of temperature with time and hydrocarbon maturation in sedimentary basins formed by extension. *Earth Planet. Sci. Lett.* **55**, 87–98.

Meissner, R. & Strehlau, J. 1982 Limits of stresses in continental crusts and their relation to the depth–frequency distribution of shallow earthquakes. *Tectonics* **1**, 73–89.

Newman, R. B. 1992 Mechanics of sedimentary basin extension. DPhil dissertation, University of Oxford, UK.

Newman, R. & White, N. 1997 Rheology of the lithosphere inferred from sedimentary basins. *Nature* **385**, 621–624.

Paterson, M. S. 1987 Problems in the extrapolation of laboratory rheological data. *Tectonophys.* **133**, 33–43.

Royden, L. & Keen, C. E. 1980 Rifting processes and thermal evolution of the continental margin of Eastern Canada determined from subsidence curves. *Earth Planet. Sci. Lett.* **51**, 343–361.

Ruppel, C. 1995 Extensional processes in continental lithosphere. *J. Geophys. Res.* **100**, 24 187–24 215.

Sawyer, D. S. 1985 Brittle failure in the upper mantle during extension of continental lithosphere. *J. Geophys. Res.* **90**, 3021–3025.

Scholz, C. H. 1990 *The mechanics of earthquakes and faulting*. Cambridge University Press.

Sclater, J. G. & Christie, P. A. F. 1980 Continental stretching: an explanation of the post-mid-Cretaceous subsidence of the central North Sea basin. *J. Geophys. Res.* **85**, 3711–3739.

Smith, D. E., Kolenkiewicz, R., Robbins, J. W., Dunn, P. J. & Torrence, M. H. 1994 Horizontal crustal motion in the central and eastern Mediterranean inferred from satellite laser ranging measurements. *Geophys. Res. Lett.* **21**, 1979–1982.

Sonder, L. J. & England, P. C. 1989 Effects of a temperature-dependent rheology on large-scale continental extension. *J. Geophys. Res.* **94**, 7603–7619.

Sonder, L. J., England, P. C., Wernicke, B. P. & Christiansen, R. L. 1987 A physical model for Cenozoic extension of western North America In *Continental extensional tectonics* (ed. M. P. Coward, J. F. Dewey & P. L. Hancock). *Geol. Soc. Lond.* (Spec. Publ.) **28**, 187–202.

Thatcher, W. 1995 Microplate versus continuum descriptions of active tectonic deformation. *J. Geophys. Res.* **100**, 3885–3894.

White, N. 1993 Recovery of strain rate variation from inversion of subsidence data. *Nature* **366**, 449–452.

White, N. 1994 An inverse method for determining lithospheric strain rate variation on geological timescales. *Earth Planet. Sci. Lett.* **122**, 351–371.

White, N. & McKenzie, D. 1988 Formation of the 'steer's head' geometry of sedimentary basins by differential stretching of the crust and mantle. *Geology* **16**, 250–253.

Discussion

W. R. Buck (*Lamont-Doherty Earth Observatory, Palisades, NY, USA*). I completely agree with Dr White's approach that data should drive anything that we're doing, and I think he has found a very interesting relationship here. He passed fairly quickly over the secondary rifting, and I didn't understand why those data so strongly support this idea of the cessation of extension being caused by strengthening because, thinking very simplistically about it, I would think that if an area extended and then stopped extending, because it got stronger, that subsequently that would not be the preferred place to rift. But he seems to be indicating the contrary, so I did not understand his argument about the implications of that data.

N. White. Figure 9 shows that the largest secondary events tend to occur where the first event is small. Similarly, where the first event is large, the second event tends to be small. Within a basin, therefore, those areas that have extended most are not the preferred sites for subsequent rifting. As you suggest, this is consistent with the lithosphere being strengthened by extension. A slightly different question is why secondary rifting should occur within the earlier basin at all, instead of in a previously unextended region. There are several possible answers. One is that although the existing basin has strengthened, it is still weaker than the surrounding continental regions. The blanketing effect of post-rift sediments may help to limit the amount of lithospheric strengthening that can occur. A second possibility is that the driving force for extension is sufficiently localized that it is much greater within the existing basin than outside it. Sometimes, extension may indeed occur outside the pre-existing basin but, if the stretching factors are small, it may be harder to detect extension there than in the basin.

K. Gallagher (*Imperial College, University of London, UK*). Just looking at the fits to the subsidence data, the variations in strain rate seem to reflect inflection points in the subsidence curve, i.e. these correlate closely to the kicks in strain rate, don't they?

N. White. Yes. The quality of the subsidence data also governs how well strain rate can be resolved.

K. Gallagher. Does he think there is information on the strain rate history in the thermal subsidence? If not, the thermal subsidence part could be thrown out and the nick points just used to infer the strain rate from the syn-rift sequence.

N. White. You can carry out this approximation, but we think that it is better to invert the subsidence data without making *a priori* assumptions about what is and what is not thermal subsidence. This more general approach safeguards against problems such as poor well location (e.g. on crests of large tilted blocks), as well as generating more confidence in what can and cannot be fitted. You also find that there are variations within the syn-rift period itself which would not be resolved using a 'nick-point' approach.

K. Gallagher. So is all the information contained in the syn-rift sequence?

N. White. All information about strain rate is necessarily contained within syn-rift periods. When modelling, you don't assume that you know when post-rift subsidence occurs, you simply let the algorithm decide where to reduce the strain rate down to zero.

A. B. Watts (*University of Oxford, UK*). Am I right in understanding that you are making use of all the information in the backstripped subsidence curves, all the bumps and ups and downs, even in a basin that has perhaps been influenced by a bit of orogeny?

N. White. Yes. The danger in using an automated approach is that variations in the rate of subsidence caused by, for example, foreland loading could be mistakenly interpreted as rift episodes. It is essential that independent evidence for the existence of rifting is used to corroborate the results of our strain rate inversions. In the basins that we have discussed here, we have paid particular attention to this issue and are confident that we can discriminate between rift episodes and other events.

D. McKenzie (*Bullard Laboratories, University of Cambridge, UK*). I want to ask Dr Gallagher's question but a little more pointedly. Dr White is using some sort of regularization to make the model smooth. If you had instantaneous extension, it would therefore be modelled with a finite extension rate because of the regularization.

N. White. I've never tried that out, but what you say must be correct, although it is an extreme case.

D. McKenzie. Dr White made quite a point of the maximum extension rate, and I agree with you that the modelling clearly has to give a maximum extension rate. The question is whether the value is well constrained by the data? Putting Dr Gallagher's point more pointedly, I don't think it is.

N. White. We have carried out synthetic tests to check the effects of different degrees of smoothing. Our results show that the maximum strain rate can be constrained to within about one-half of an order of magnitude. Should our peak strain rates be somewhat higher than we have determined, then our conclusion about the importance of dry olivine rheology controlling the mechanics of extension would still hold. Present-day geodetic strain rates from areas such as the Aegean are faster than the ones we show here. We suspect that this difference is a consequence of the tectonic regime rather than a systematic error in our modelling.

D. McKenzie. I agree with Dr White as to what the fastest extension rate really is now. But I disagree that he can estimate it reliably from subsidence curves, because of the problem of regularization.

N. White. Professor McKenzie is correct, but only up to a point. The regularization does not have such an extreme effect on our results.

N. Kusznir (*University of Liverpool, UK*). The syn-rift component of subsidence is obviously controlled by faults; for example, we get uplift in the footwall. Obviously, to understand subsidence we need to understand faults as well. How does Dr White actually allow for this within his approach, which is essentially one dimensional?

N. White. In one dimension, all you can do is choose wells that are not on the crests of fault-bounded blocks greater than about 20 km in width. Fortunately, more and more wells are now being drilled within hanging walls, where the effect Professor Kusznir refers to is less important. One advantage in using an automated approach such as ours is that failure is diagnostic: when the syn-rift component is not sampled adequately, a satisfactory solution cannot be found. Of course, we would like to be able to invert in two dimensions (i.e. calculate strain rate as a function of distance and time) and thus address his concerns fully. Paul Bellingham has written a two-dimensional algorithm at Cambridge and he is testing it on data from the North Sea Basin.

N. Kusznir. If you selectively prefer hanging walls and depocentres, you can over-estimate the syn-rift subsidence component. How will that impinge on Dr White's analysis of inversion?

N. White. My answer to the previous question partly addresses this question. We do not believe that spatial sampling in one dimension is a big problem. At worst, it would make the difference between, say, 1 and $2 \times 10^{-15}\ \mathrm{s}^{-1}$, but it does not change our results by even half orders of magnitude.

A. B. Watts. Dr White assumed zero strength, in terms of the backstrip-loaded subsidence, when he backstripped all these 2000 wells. Would it not be better in future to try to constrain the local strength, perhaps using gravity or something else, and then to backstrip?

N. White. The simple answer to your question is 'yes', but I would like to qualify it with two comments. First, there's been a drive downwards in elastic thicknesses over the continents. In cratonic North America, we used to think that the elastic thickness was as great as 100 km. More recent work, using the admittance between free-air gravity anomalies and topography, rather than coherence methods, has shown that the elastic thickness is nearly one order of magnitude smaller. Secondly, at the subsidence wavelengths that we consider, the difference between Airy isostasy and an elastic thickness of 5–20 km is small. Nonetheless, when we develop two- and three-dimensional algorithms for inverting basins, it would be sensible to include elastic thickness as one of the parameters.

L. Géli (*IFREMER, France*). Can Dr White give details about the time-scale he used and the effect of timing uncertainties on his results?

N. White. The answer to this question can be divided into two parts. First, a variety of published time-scales have been tried out. Differences in time-scales do have a direct effect upon the calculated strain rate, but the variation is quite small if one is mainly concerned with order of magnitude changes in strain rate. Second, the whole point about using inversion techniques is that routine error analysis can

PHILOSOPHICAL TRANSACTIONS OF THE ROYAL SOCIETY A MATHEMATICAL, PHYSICAL & ENGINEERING SCIENCES

be carried out. As I have previously shown (White 1994), one can easily calculate the *a posteriori* covariance matrix which is strongly diagonal, thus demonstrating that different values of strain rate at different times do not trade off against each other. Alternatively, one can use the brute-force approach and perform a Monte Carlo analysis which shows how errors in the time-scale translate into errors in strain rate distribution. I believe that the results shown today are robust to within one-half order of magnitude, but I acknowledge that improvements in the absolute geological time-scale will place this kind of inverse modelling on a much sounder footing.

R. S. White (*Bullard Laboratories, University of Cambridge, UK*). All the continental rifted basins Dr White has shown exhibit beta stretching factors of less than 1.4. To form an ocean basin the stretching factor has to be greater than 5 or so. Is the population of stretching factors bimodal, with a missing gap between 1.4 and 5, or do you think that basins exist with beta factors lying across the whole range from 1 to infinity?

N. White. The continent interiors are characterized by low stretching factors, typically between 1.1 and 1.4. The problem that you refer to is a data gap rather than anything else: industry doesn't drill wells through greater than 4 km of sedimentary rock and so we effectively cannot sample stretching factors greater than 1.4. The only exceptions occur in southeast Asia where, because of the fact that rifting occurred during the Cenozoic, a 4 km deep hole can sample, in the subsidence sense, much higher betas (P. Wheeler, personal communication). Nonetheless, a form of bimodality does exist; basins with low strain rates and stretching factors are extremely common while at the other end of the spectrum highly stretched passive margins and ocean basins occur. The reasons for this distribution are discussed in our contribution.

A. B. Watts. Dr White's plot of peak strain rate against stretching factor appears to go asymptotic at about $10^{-15}\,\mathrm{s}^{-1}$. Does this constrain the maximum possible strain rate at highly extended passive margins?

N. White. We suspect that strain rates do indeed reach a maximum value of about $10^{-15}\,\mathrm{s}^{-1}$ for these kinds of basins. However, it is not yet possible to determine strain rates for the deeper portions of passive margins because of a lack of deep boreholes and because of palaeobathymetric uncertainties.

A. B. Watts. This raises an interesting question about these intracratonic basins, especially ones like the Illinois Basin, where a lot of the evidence from seismic and gravity modelling suggests that the crust is not thinnest under the Basin but actually thins away from the Basin. I wonder if Dr White would like to comment on that in terms of the general problem of intracratonic basins and the relative roles of extension and other mechanisms.

N. White. Seismic reflection data from the Illinois Basin show growth on normal faults during the Cambrian. This information corroborates the results of strain rate inversion. We infer from these two independent data-sets that the crust thinned beneath Illinois by stretching factors of 1.1–1.2 during the Early Palaeozoic. The present-day crustal thickness beneath the Basin may or may not record this amount of thinning, since we cannot rule out post-Palaeozoic modification.

A. B. Watts. Might the Moho be younger than the rifting under some of these basins?

N. White. You certainly cannot rule out small changes in crustal thickness during the 300 plus million years that have elapsed since lithospheric extension took place. Consequently, we are wary of using present-day crustal thickness variation as a direct measure of Palaeozoic thinning.

N. Kusznir. How seriously does Dr White think his subsidence data are contaminated by foreland basin subsidence, where we observe subsidence and uplift caused by many other geodynamic processes? What steps does he take to try to remove that problem?

N. White. It would be very foolish to invert a large quantity of subsidence data without paying attention to other geological observations which have a bearing on the problem. In each of the regions that we have analysed, we have used information about normal faulting and magmatism to help constrain rift episodes. A good example is the Timan–Pechora Basin in the former Soviet Union which is located close to the Ural Mountains. As you approach the Urals, flexural bending occurred as a result of Uralian Mountain loading. Thus close to the Urals it is clear that you get Permian–Triassic foreland loading. You cannot model this subsidence event using an extensional model because the subsidence gradient cannot be fitted regardless of the value of beta. As you move westward, however, there is evidence that foreland basin subsidence stops and you observe extension. This Permian–Triassic extension episode is well documented. The area between foreland loading and extension is more difficult to model. It is very important to be aware of this type of regional variation when you model subsidence data.

PHILOSOPHICAL TRANSACTIONS OF THE ROYAL SOCIETY A MATHEMATICAL, PHYSICAL & ENGINEERING SCIENCES